Chinese Journal of Catalysis 37 (2016) 1413–1422

available at www.sciencedirect.com

ScienceDirect

journal homepage: www.elsevier.com/locate/chnjc

Article

Changing the balance of the MTO reaction dual-cycle mechanism: Reactions over ZSM-5 with varying contact times

Mozhi Zhang [a,c], Shutao Xu [a], Yingxu Wei [a,#], Jinzhe Li [a], Jinbang Wang [a], Wenna Zhang [a,c], Shushu Gao [a,c], Zhongmin Liu [a,b,*]

[a] *National Engineering Laboratory for Methanol to Olefins, Dalian National Laboratory for Clean Energy, iChEM (Collaborative Innovation Center of Chemistry for Energy Materials), Dalian Institute of Chemical Physics, Chinese Academy of Sciences, Dalian 116023, Liaoning, China*

[b] *State Key Laboratory of Catalysis, Dalian Institute of Chemical Physics, Chinese Academy of Sciences, Dalian 116023, Liaoning, China*

[c] *University of Chinese Academy of Sciences, Beijing 100049, China*

ARTICLE INFO

Article history:
Received 4 May 2016
Accepted 17 May 2016
Published 5 August 2016

Keywords:
Methanol to olefins
Dual-cycle mechanism
ZSM-5
Contact time
Hydrogen transfer reaction

ABSTRACT

The methanol to olefins (MTO) reaction was performed over ZSM-5 zeolite at 300 °C under various methanol weight hourly space velocity (WHSV) values. During these trials, the catalytic performance was assessed, in addition to the formation and function of organic compounds retained in the zeolite. Analysis of reaction effluents and confined organics demonstrated a dual-cycle reaction mechanism when employing ZSM-5. The extent of the hydrogen transfer reaction, a secondary reaction in the MTO process, varied as the catalyst-methanol contact time was changed. In addition, $^{12}C/^{13}C$-methanol switch experiments indicated a relationship between the dual-cycle mechanism and the extent of the hydrogen transfer reaction. Reactions employing a low methanol WHSV in conjunction with a long contact time favored the hydrogen transfer reaction to give alkene products and promoted the generation and accumulation of retained organic species, such as aromatics and methylcyclopentadienes, which enhance the aromatic cycle. When using higher WHSV values, the reduced contact times lessened the extent of the hydrogen transfer reaction and limited the generation of methylcyclopentadienes and aromatic species. This suppressed the aromatic cycle, such that the alkene cycle became the dominant route during the MTO reaction.

1. Introduction

The methanol-to-hydrocarbons process was first discovered and investigated by Chang et al. [1,2] in the 1970s. After several decades of research, the methanol-to-olefins (MTO) process has been developed as an alternative non-petrochemical route to the production of light olefins from coal via methanol, and this technique is currently employed on an industrial scale [3,4].

Fundamental research into the MTO reaction mechanism has proceeded simultaneously with this industrial utilization [5,6], and more than 20 distinct reaction mechanisms have been proposed to explain the direct formation of C–C bonds from C_1 species such as methanol or dimethyl ether (DME) [7–11]. However, these direct C–C formation mechanisms are unlikely, due to the high associated energy barriers [12–14]. Dahl et al. [15–17] have put forward an alternative, indirect

* Corresponding author. Tel: +86-411-84379335; Fax: +86-411-84691570; E-mail: liuzm@dicp.ac.cn
# Corresponding author. Tel: +86-411-84379118; Fax: +86-411-84691570; E-mail: weiyx@dicp.ac.cn

This work was supported by the National Natural Science Foundation of China (91545104, 21576256, 21473182, 21273230, 21273005) and the Youth Innovation Promotion Association of the Chinese Academy of Sciences.
DOI: 10.1016/S1872-2067(16)62466-X | http://www.sciencedirect.com/science/journal/18722067 | Chin. J. Catal., Vol. 37, No. 8, August 2016

C–C formation mechanism, the so-called hydrocarbon-pool mechanism, that bypasses these high energy barriers, based on computational simulations and experimental data, and this mechanism is now generally accepted [18–23].

Because it is an excellent catalyst for the MTO reaction to produce light olefins, the MTO mechanism over ZSM-5 zeolite has been intensively investigated by many researchers [24–32]. In 2006, Svelle et al. [33] found inconsistencies in the ^{13}C contents of ethene and other higher alkenes when carrying out $^{12}C/^{13}C$-methanol switch trials over ZSM-5, and proposed that ethene formation was generated by a different mechanism than the other, higher alkenes. Soon after, they proposed a dual-cycle mechanism consisting of aromatic and alkene cycles to explain the inconsistent ethene and higher alkene data [34]. Other studies have found similar evidence of a dual-cycle mechanism and examined the properties of the two cycles in MTO reactions over different zeolites [35–37].

Scheme 1 summarizes the dual-cycle mechanism, which can be regarded as the combination of an aromatic cycle and an alkene cycle. In the aromatic cycle, for both paring and side-chain routes, methylcyclopentenyl (MCP^+) and polymethyl-benzenium ($polyMB^+$) cations are the primary active intermediates [24,25,38]. In the case of the alkene cycle, involving alkene methylation and cracking, C_3 to C_7 straight chain alkenes predominate [39–41].

The formation and reaction of MCP^+ and $polyMB^+$ cations and the deprotonated forms of these same compounds (Scheme 2) represent the key evidence for the aromatic cycle. Using solid-state magic angle spinning (MAS) NMR, several highly active carbenium cations, including MCP^+ and $polyMB^+$, have been successfully detected in zeolites. The generation and transformation of these species has been studied in detail so as to elucidate their important roles in the MTO reaction, using several zeolites such as ZSM-5, SSZ-13, SAPO-34 and Beta [24,37,38].

In the case of zeolites that do not favor the generation and accumulation of bulky cyclic species, such as ZSM-22, very low amounts of methylcyclopentadienes and aromatic species are generated compared with the amounts produced by SSZ-13, SAPO-34 and Beta zeolites. However, the MTO reaction still proceeds over ZSM-22, and primarily produces C_3–C_7 straight chain alkenes. In addition, $^{12}C/^{13}C$-methanol switch experiments indicate very low participation of bulky cyclic species in the reaction. The MTO reaction over ZSM-22 leads to a very high ^{13}C content in the resulting alkenes, and so can be considered to be almost completely dependent on the alkene cycle to convert methanol and produce olefins [40,41].

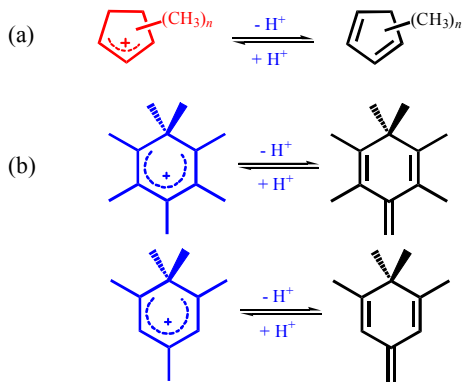

Scheme 2. (a) The MCP^+ cation and its deprotonated form, the substituted methylcyclopentadienes; (b) The $polyMB^+$ cation and its deprotonated form, polymethylmethylenecyclohexadiene.

The dual-cycle mechanism is not just a simple addition of two cycles, but rather an integrated collective in which the two cycles significantly affect one another. As an example, the olefin products from the aromatic cycle can function as active intermediates during the alkene cycle. Another connection between the two cycles is the hydrogen transfer reaction, which is a secondary reaction in the MTO process and primarily converts higher olefins in the alkene cycle to hydrogen-rich alkanes and hydrogen-poor cyclic species such as methylcyclopentadienes and aromatics in the aromatic cycle [34,42,43].

In the present study, methanol conversion was performed over ZSM-5 zeolite at 300 °C as a means of studying the dual-cycle mechanism of the MTO reaction. Analyses of the effluent products as well as the species retained in the zeolite, in addition to $^{12}C/^{13}C$-methanol switch experiments, were con-

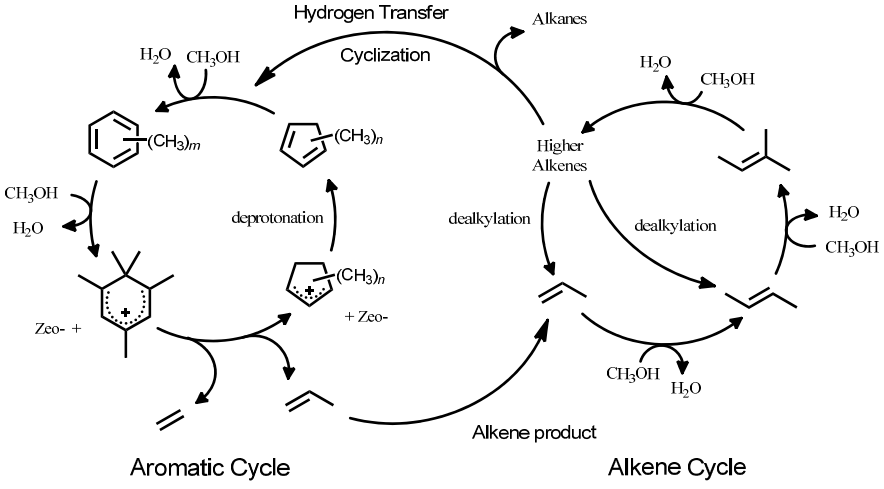

Scheme 1. The dual-cycle mechanism of the MTO reaction.

ducted to assess the relative predominance of the aromatic cycle or alkene cycle mechanism at different WHSV values and contact times. The data indicate that varying the reaction conditions during the MTO reaction over ZSM-5 can emphasize one reaction route over another.

2. Experimental

2.1. Catalyst characterization

The ZSM-5 zeolite used in this work was an NKF-5 zeolite in the H-form, purchased from the Catalyst Plant of Nankai University. This material was applied as the catalyst for MTO reactions after being calcined at 550 °C for 3 h.

The powder X-ray diffraction (XRD) pattern of the ZSM-5 zeolite was obtained using a PANalytical X'Pert PRO X-ray diffractometer with Cu K_α radiation (λ = 1.5418 Å), operating at 40 kV and 40 mA. N_2 adsorption-desorption data were acquired with a Micromeritics ASAP 2020 physical adsorption analyzer at –196 °C. The crystal size and morphology of the zeolite were assessed by field emission scanning electron microscopy (FE-SEM, Hitachi, SU8020), and the chemical composition was determined using a Philips Magix-601 X-ray fluorescence (XRF) spectrometer.

The ^{29}Si, ^{27}Al and ^{1}H MAS NMR spectra of the ZSM-5 zeolite were recorded on a Bruker Avance III 600 spectrometer using a 4-mm MAS probe, at respective resonance frequencies of 119.2, 156.4 and 600.13 MHz. ^{29}Si MAS NMR spectra were acquired at a spinning rate of 6 kHz using high-power proton decoupling, accumulating 1024 scans with a π/4 pulse width of 2.5 μs and a 10-s recycle delay. Chemical shifts were referenced to 4,4-dimethyl-4-silapentane sulfonate sodium salt (DSS) at 0 ppm. ^{27}Al MAS NMR spectra were obtained at a spinning rate of 12 kHz using a single pulse sequence, and 600 scans were accumulated with a π/8 pulse width of 0.75 μs and a 2-s recycle delay. Chemical shifts were referenced to $(NH_4)Al(SO_4)_2{\cdot}12H_2O$ at –0.4 ppm. Prior to ^{1}H MAS NMR experiments, the zeolite was dehydrated at 400 °C at a pressure below 10^{-3} Pa for 20 h. ^{1}H MAS NMR spectra were acquired using a single pulse sequence with a π/4 pulse of 2 μs and a 10-s recycle delay, with adamantane (1.74 ppm) as the chemical shift reference. The sample was weighed to allow for quantification of the Brönsted acid site density, and the ^{1}H MAS NMR spectrum was resolved using the Dmfit software package in conjunction with Gaussian-Lorentz line shapes, using adamantane (1.74 ppm) as the quantitative external standard, with a spectrum acquired under the same NMR conditions [37,44,45].

2.2. Methanol-to-hydrocarbons conversion

The ZSM-5 zeolite was pressed, broken into pieces and then sieved to obtained particles with sizes ranging from 40 to 60 mesh. Prior to the reaction, a quantity of the catalyst (50 to 100 mg) was loaded into a stainless steel tube reactor with an inner diameter of 5 mm and activated at 500 °C under flowing N_2 (25 mL/min) for 40 min, after which the reactor was heated to 300 °C in preparation for the reaction. $^{13}CH_3OH$ was fed into the reactor by passing a carrier gas (25 to 129 mL/min) through a saturator containing methanol held at 5 to 14 °C, giving WHSV values of 2 to 12 h^{-1}. All reactions were performed under atmosphere pressure. The effluent exiting the reactor was maintained at 200 °C and subsequently analyzed via online gas chromatography (GC), using a PoraPLOT-Q capillary column and a flame ionization detector (FID) in conjunction with mass spectrometry (MS, Agilent 7890B/5977A). The extent of methanol conversion and the selectivities for various products were calculated on a CH_2 basis, considering DME as a reactant [46,47].

2.3. $^{12}C/^{13}C$-methanol switch experiments

In the $^{12}C/^{13}C$-methanol switch experiments, ^{12}C-methanol was initially fed into the reactor for some time, after which the feed flow, which had passed through a saturator containing ^{12}C-methanol, was quickly switched to pass through a saturator holding ^{13}C-methanol and this scenario was maintained for an additional 0.5–3 min [46]. The isotopic distributions of the effluents were analyzed using the same online GC-MS instrumentation described in Section 2.2. Following the reaction, the reactor was rapidly quenched with liquid nitrogen to stop the reaction and the catalysts were discharged for analysis, as described in Section 2.4.

2.4. Confined organics determination with GC-MS

After the reaction, the catalyst was quickly cooled, discharged from the reactor, transferred into a Teflon vial, and dissolved in 20 wt% HF over 1 h. Following complete dissolution, the solution was neutralized with 7 wt% aqueous KOH, and CH_2Cl_2 was added to the vial to extract the chemical species retained in the catalyst. The CH_2Cl_2 phase was subsequently analyzed by GC-FID-MS (Agilent 7890A/5975C) using an HP-5 capillary column [48,49]. Hexachloroethane was employed as an internal standard for quantification and the NIST11 mass spectral library was used to determine the identities of the various analytes.

3. Results and discussion

3.1. Catalyst characterization

The powder XRD pattern of the catalyst is provided in Fig. 1 and demonstrates the high purity and crystallinity of the ZSM-5 zeolite. The SEM image in Fig. 2 indicates a hexagonal morphology and an average crystal size of approximately 1.5 μm.

The ^{29}Si MAS NMR spectrum obtained from the ZSM-5 (Fig. 3(a)) indicates Si atoms in several different chemical environments: Q^3, Si(1Al) and two nonequivalent crystallographic Q^4 sites [45]. The framework Si/Al ratio, calculated by deconvolution of the ^{29}Si MAS NMR spectrum according to Loewenstein's rule [50], was 19.0, reasonably close to that determined from XRF (17.9). The ^{27}Al MAS NMR spectrum (Fig. 3(b)) shows that the majority of the Al atoms were in the framework tetrahedral coordination state. The ^{1}H MAS NMR spectrum (Fig. 3(c)) ex-

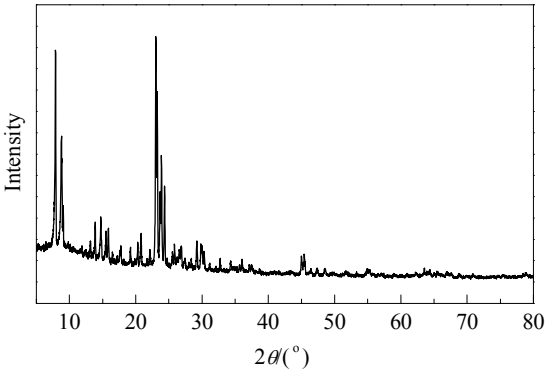

Fig. 1. XRD pattern obtained from the ZSM-5 zeolite.

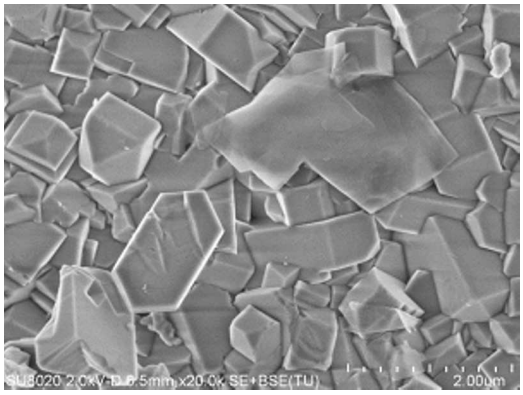

Fig. 2. SEM image of the ZSM-5 zeolite.

hibits peaks at 5.7, 3.8, 2.5 and 1.7 ppm, respectively attributed to bridge hydroxyl groups with hydrogen bonding and acting as Brönsted acid sites, bridge hydroxyl groups acting as Brönsted acid sites, aluminum hydroxyl groups with hydrogen bonding, and silicon hydroxyl groups [45,51]. The Brönsted acid site density was determined to be 0.77 mmol/g by quantifying the amounts of both types of bridge hydroxyl groups based on their signal intensities, using adamantane as an external standard. Based on N_2 adsorption-desorption data, the BET surface area and *t*-plot micropore volume of the ZSM-5 sample were 355 m^2/g and 0.124 cm^3/g, respectively.

3.2. Conversion and product selectivities during the MTO reaction

Fig. 4 summarizes the effluent analysis data acquired during MTO reactions over the ZSM-5 at 300 °C. The methanol WHSV values 2, 6 and 12 h^{-1} correspond to reactions performed with catalyst-reactant contact times of 156, 32 and 16 ms, respectively. At the lowest WHSV of 2 h^{-1}, the methanol conversion was only 1.4% at a time on stream (TOS) of 5 min, and the products were primarily C_2 to C_6, along with a substantial

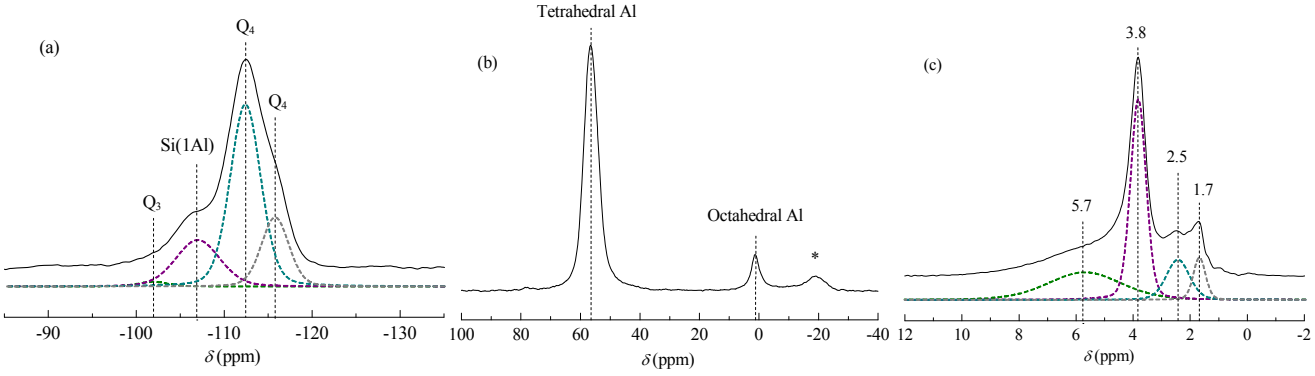

Fig. 3. ^{29}Si (a), ^{27}Al (b) and ^{1}H (c) MAS NMR spectra of ZSM-5, with fitted peaks indicated. The asterisk in (b) indicates a sideband.

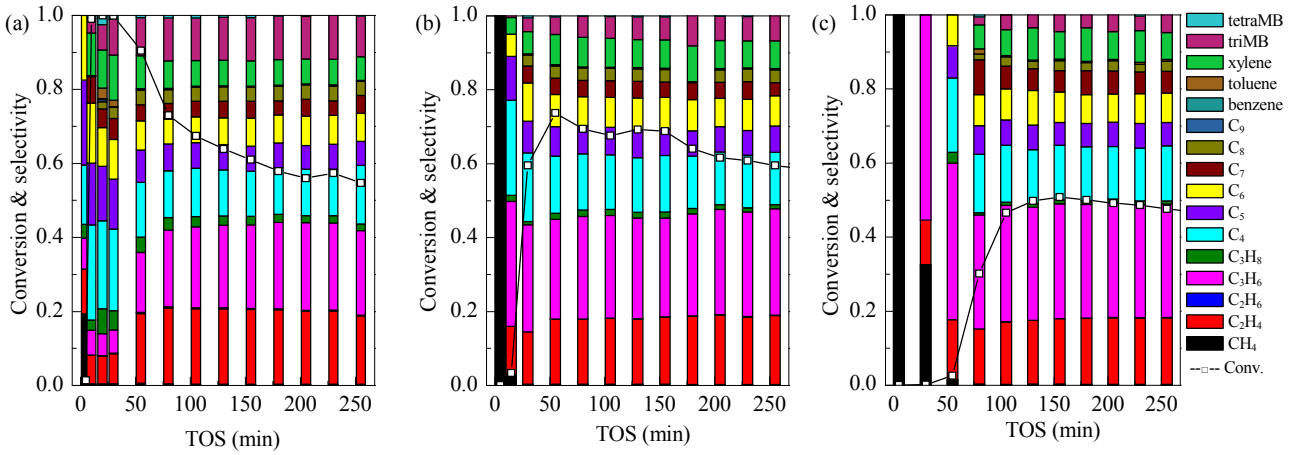

Fig. 4. Conversions and product distributions during the MTO reaction over ZSM-5 at 300 °C and different WHSV values. (a) 2 h^{-1}; (b) 6 h^{-1}; (c) 12 h^{-1}.

amount of methane. At TOS = 20–30 min, the reaction resulted in 100% methanol conversion and high selectivities for the relatively heavier C_4 to C_8 components and xylene. However, after reaction of 30 min, the methanol conversion gradually declined from 100% to approximately 55% at TOS = 255 min, accompanied by a decrease in the selectivities for C_4 to C_7 and an increase in the selectivities for ethene, propene and trimethylbenzene. At higher WHSV values of 6 and 12 h^{-1}, the reaction exhibited an induction period and the methanol conversion increased in an "S" curve, which is typical of an autocatalytic reaction. Careful comparison of the data indicates that at higher WHSV values the induction period was increased, to 55 min at 6 h^{-1} and 105 min at 12 h^{-1}, and the maximum conversion at each of these WHSV values dropped, from 74% to 50%. At the beginning of the induction period, the hydrocarbon products were primarily low-carbon species, such that only methane was detected at TOS = 5 min at 6 and 12 h^{-1}, suggesting the deposition of hydrogen-poor species such as aromatic compounds in the zeolite pores. As the reaction proceeded, similar to the results obtained at 2 h^{-1}, heavier species emerged among the effluents, and greater selectivity was observed for ethene, propene and various aromatics. After the induction period, the reaction seems to have stabilized, and the conversion and product selectivities remained relatively constant.

Comparing the reactions at the three different methanol WHSV values, there is a negative correlation between the maximum methanol conversion and the WHSV. It is easy to understand that when using a constant amount of catalyst, as more methanol is supplied, there will be greater amounts of unconverted methanol and thus a lower maximum conversion rate. With regard to the selectivities for the gas phase products, although reactions of the three different WHSV values all produced primarily ethene, propene, butene and aromatics during the stable reaction time period, slight differences were still evident. During the low WHSV (2 h^{-1}) reaction, more ethene and aromatics were generated, while the higher WHSV (6 or 12 h^{-1}) reactions resulted in higher selectivities for propene and butene. In addition, there was less formation of propane and other alkanes during the high WHSV reactions. The hydrogen transfer index (HTI) values, defined as the C_3H_8/C_3H_6 selectivity ratios, are plotted as functions of TOS in Fig. 5. These data indicate the significantly promoted hydrogen transfer reaction at a low WHSV and a long contact time, and in contrast, the hydrogen transfer reaction is largely suppressed at high WHSV reactions. These variations in the selectivity imply that the reactions follow different routes when applying different methanol WHSV values.

3.3. GC-MS study of retained organic species in the zeolite

According to the indirect C–C bond formation mechanism, the MTO reaction requires hydrocarbon-pool species to perform the methanol conversion to olefins. The organic species retained in the catalyst therefore play a very important role in the overall reaction. During the induction period, the gradual generation and accumulation of organic species in the zeolite transforms the original material to an efficient working catalyst. Following this induction period, the methanol conversion reaches a maximum and almost all the methanol conversion and olefin production occurs with the aid of these retained organic species, acting as important intermediates. As such, the mechanism of the MTO process is closely associated with the hydrocarbon-pool species in the zeolite, and the analysis of these retained organic species should provide helpful information regarding the effects of the various WHSV values on the reaction mechanism.

3.3.1. Retained polymethylbenzene species in the zeolite

During the induction period, the concentrations of retained active species were increased, leading to the maximum conversion at the end of the induction period. At this point, there should be few retained inert organic species on the highly reactive catalyst and so, following methanol conversion at TOS = 20 min (WHSV = 2 h^{-1}), TOS = 55 min (WHSV = 6 h^{-1}) and TOS = 105 min (WHSV = 12 h^{-1}), the discharged catalysts were dissolved in HF and the organic species were extracted with CH_2Cl_2 and analyzed via GC-MS. Fig. 6 show that the primary retained species at the different WHSV values were

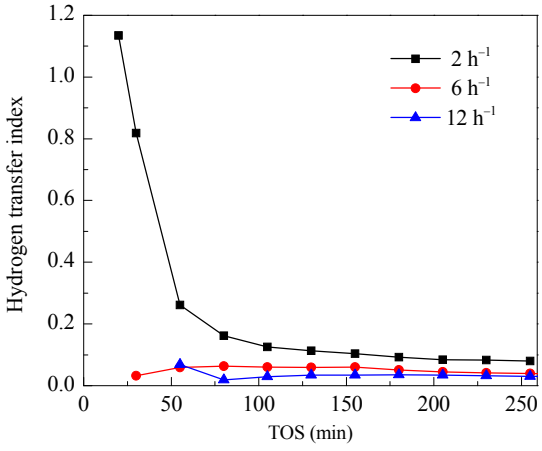

Fig. 5. Hydrogen transfer indexes (the C_3H_8/C_3H_6 selectivity ratios) of MTO reactions over ZSM-5 at 300 °C with different methanol WHSV values, as functions of TOS.

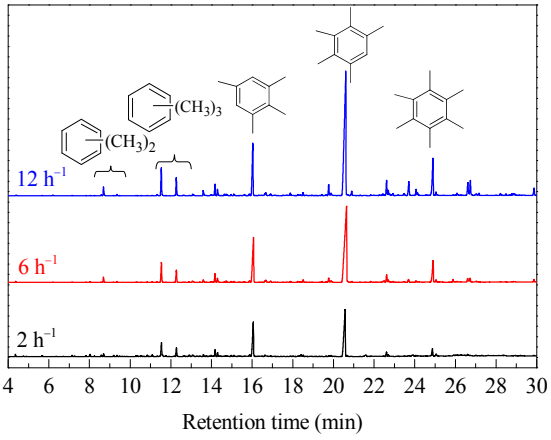

Fig. 6. GC-MS analysis of the extracted organics retained in zeolites after methanol conversion at TOS = 20 min (WHSV = 2 h^{-1}), TOS = 55 min (WHSV = 6 h^{-1}) and TOS =105 min (WHSV = 12 h^{-1}).

polymethylbenzenes, and in each case there is a similar distribution, with pentamethylbenzene (pentaMB) and tetramethylbenzene (tetraMB) as the main aromatics together with relatively small amounts of hexamethylbenzene (hexaMB), trimethylbenzene (triMB) and xylene.

These polymethylbenzene species, which are important active retained organic species in the MTO reaction, are generated via secondary reactions of olefin products, including oligomerization, cyclization and hydrogen transfer [24,34]. Although these aromatics are generated and accumulated as the reaction proceeds at all WHSV values, there are still variations in the rate of aromatics accumulation. When the hydrogen transfer reaction is pronounced, the aromatics tend to be generated more rapidly and accumulate in the zeolite to a greater extent as the methanol is consumed, and vice versa. Thus the accumulation rate of aromatics, to some extent, reflects the extent of secondary reactions, especially the hydrogen transfer reaction, just as in the HTI comparison in Fig. 5.

The results in Fig. 6 show the retained organic species accumulated in the zeolite. However, the amounts of aromatic species were obtained while applying different WHSV values and reaction times, meaning that the catalysts were exposed to different amounts of methanol feed. For this reason, the peak integration values of several aromatics were used to determine the average accumulation rates at various methanol feeds, with the results provided in Fig. 7. These data allow the accumulation rates from reactions with different WHSV values to be directly compared. From Fig. 7, it can be obtained that those reactions with lower WHSV and longer contact time exhibit much higher aromatic accumulation rates. As noted, the generation and accumulation rates of these aromatics can be used to assess the extent to which the hydrogen transfer reaction occurs. The rapid accumulation of aromatics demonstrates the rapid progression of the hydrogen transfer reaction at the lowest WHSV and longest contact time. In contrast, a high WHSV and short contact time obviously restrict the generation of aromatics and severely suppress the hydrogen transfer reaction.

3.3.2. *Retained methylcyclopentadiene species in the zeolite*

In addition to polymethylbenzene species, MCP^+ ions are also important active intermediates in the MTO reaction over ZSM-5. Haw et al. [24] and Wang et al. [30,32] demonstrated the existence of several alkyl isomers of MCP^+ and their deprotonated neutral form, MCP. In the present study, MCP species were detected during the GC-MS analysis of retained species (Fig. 6), although the concentrations of these compounds were very low and sometimes obscured by the high concentrations of methylbenzenes. To remove the interference of the methylbenzenes, extracted ion chromatograms were obtained during analysis of the retained species, at m/z = 94, 108, 122 and 136, representing dimethylcyclopentadiene (diMCP), trimethylcyclopentadiene (triMCP), tetramethylcyclopentadiene (tetraMCP) and pentamethylcyclopentadiene (pentaMCP) and their isomers, respectively. These are presented in Fig. 8.

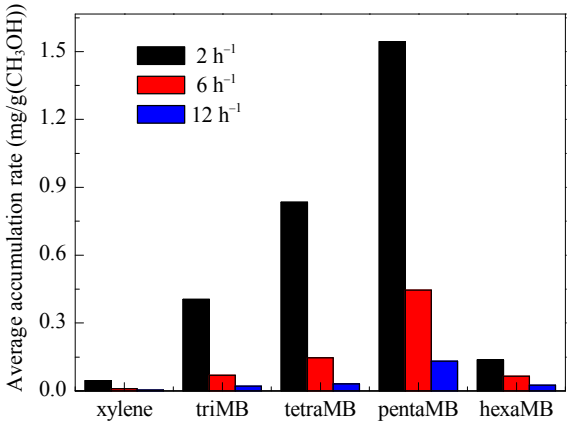

Fig. 7. Average accumulation rates of retained aromatics at various WHSV values.

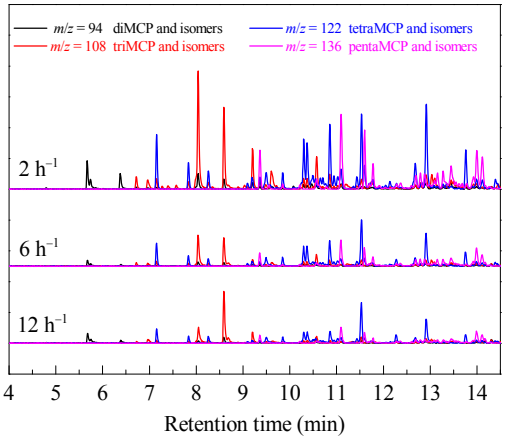

Fig. 8. Extracted ion chromatograms (EIC) at m/z = 94, 108, 122 and 136 from the GC-MS analysis data for retained species in the zeolite in Fig. 6 following methanol conversion at various WHSV values.

From Fig. 8, it is evident that there are four types of retained MCP species obtained at different WHSV values and that their distributions are very similar. However, there are some small variations in the amounts. In the reaction with a low WHSV (2 h^{-1}), the peak areas of almost all the MCP species in the zeolite are greater than those obtained using higher WHSV values (6 or 12 h^{-1}), even though the reaction time at the low WHSV was 20 min, and therefore much shorter than the 55- and 105-min time spans of the high WHSV reactions. Thus, the average rate at which MCP species accumulated when employing a low WHSV and a long contact time definitely exceeded those in the reactions with a high WHSV and short contact time. Similar to the polymethylbenzenes data, the generation and accumulation of these MCP species were also affected by the extent of the hydrogen transfer reaction. Judging from both the total amounts and the above estimates of the average accumulation rates at various methanol feeds, the formation of MCP species is even more sensitive to the WHSV and the catalyst-methanol contact time than is the formation of polymethylbenzenes.

3.4. *MTO reaction mechanisms from $^{12}C/^{13}C$-methanol switch experiments*

The dual-cycle mechanism for MTO reactions over ZSM-5

was first proposed by Svelle et al. [33] and Bjørgen et al. [34] in 2006, and consists of aromatic and alkene cycles. The aromatic cycle involves MCPs and aromatics as active intermediates, while the alkene cycle primarily consists of alkene chain generation in conjunction with alkene methylation and cracking. The alkene products from the aromatic cycle can be regarded as intermediates that subsequently promote the alkene cycle. Simultaneously, the hydrogen transfer reaction transforms the higher chain alkenes generated in the alkene cycle to aromatics, which in turn promotes the aromatic cycle. In this way, the two cycles affect and interact with one another.

$^{12}C/^{13}C$-methanol switch experiments are widely used in the study of the MTO reaction to track the destination of ^{13}C atoms from methanol and so to elucidate the reaction route during methanol conversion. This technique also allows one to distinguish the active organic species and to determine their roles in the overall reaction. In this study, $^{12}C/^{13}C$-methanol switch trials were carried out with different WHSV values, and the total ^{13}C contents of the effluent alkenes and retained organics after the switch experiments are shown in Fig. 9.

For the reaction performed at a low WHSV (2 h^{-1} in Fig. 9(a)), the ^{13}C contents of the C_3–C_6 alkenes and xylene were approximately 30% at a switch time of 2 min, while the ^{13}C content of the ethene was very high (up to 70%). In the case of the retained organic species, the pentaMB had the highest ^{13}C content, 70% at a switch time of 2 min, with ^{13}C contents of about 50% for the tetraMB, hexaMB, tetraMCP and pentaMCP. With the exception of the triMB, the ^{13}C contents of the retained organic species were close to those of the effluent species under low WHSV (2 h^{-1}).

The data obtained from the reactions with higher WHSV values (6 h^{-1} in Fig. 9(b) and 12 h^{-1} in Fig. 9(c)) indicate that, although the pentaMB still had the highest ^{13}C content (approximately 50%) among the retained species, the ^{13}C contents of all the retained species were lower compared with those obtained at a WHSV of 2 h^{-1}. At the same time, with the exceptions of ethene and xylene, the ^{13}C contents of the effluent alkenes increased substantially, from 30%–40% at a WHSV of 2 h^{-1} to 70%–90% at WHSV values of 6 and 12 h^{-1}. These opposing changes resulted in pronounced differences in the ^{13}C contents of the effluent alkenes and retained compounds at WHSV values of 6 and 12 h^{-1}. In addition, the ethene ^{13}C content of 65% was significantly lower than the 70%–90% levels in the C_3–C_6 alkenes in the reactions performed at WHSV values of 6 or 12 h^{-1}, which is the opposite to the results obtained at the low WHSV.

Typically, a higher ^{13}C content in an organic species indicates greater participation of this species in the reaction process and demonstrates that the conversion route that produces this species is highly active. In the case of the low WHSV reaction, the ^{13}C contents of the effluents and retained organic species were similar, meaning that the production of the effluent alkenes was strongly linked to the presence of the retained species. Considering the participation of retained species in the aromatic cycle of the dual-cycle mechanism, it is evident that the aromatic cycle was undoubtedly predominant during the low WHSV reaction. The alkene cycle is typically responsible for the generation of propene, butene and other higher alkenes. Conversely, the production of ethene is almost completely dependent on the aromatic cycle, and so the high ^{13}C content of the ethene also demonstrates the high activity of the aromatic cycle during the low WHSV reaction.

The higher WHSV (6 or 12 h^{-1}) reactions generated alkenes with ^{13}C contents that were higher than those of the retained organic species. Therefore, the aromatic cycle only contributed partly to the MTO activity and the alkene cycle must also have proceeded during methanol conversion at the same time. The alkene cycle utilizes gas phase C_3 to C_7 alkenes as active intermediates and does not required the retained species in the catalyst, and so the difference in the ^{13}C contents of the effluent alkenes and retained species obviously indicates the important role of the alkene cycle in the higher WHSV reactions. In addition, the lower ^{13}C content of ethene compared to those of the higher alkenes also suggests the major role of the alkene cycle. In general, during the MTO reaction over ZSM-5, low WHSV conditions favor the aromatic cycle while high WHSV conditions promote the alkene cycle.

Although the production of alkenes is the main reaction

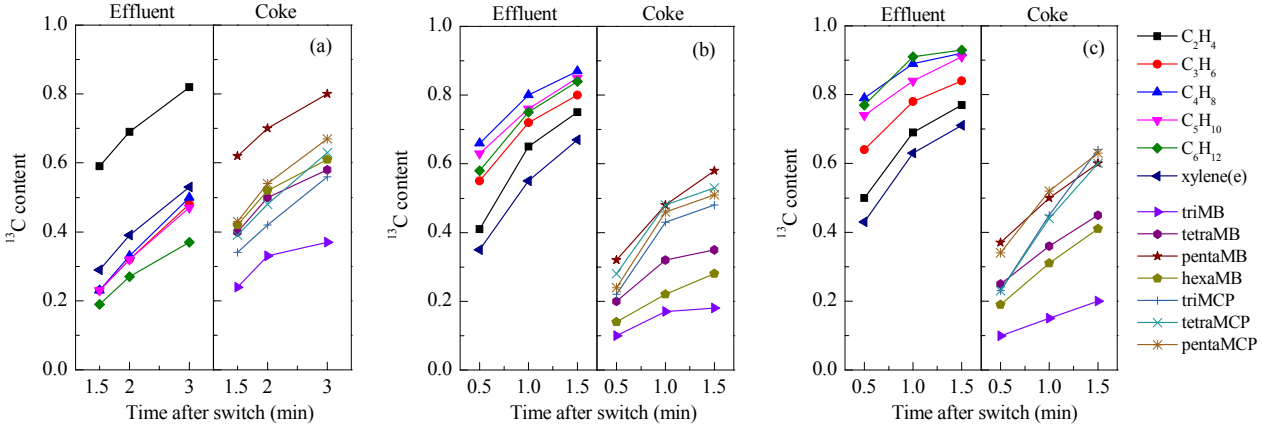

Fig. 9. ^{13}C contents of effluents and retained organic species from $^{12}C/^{13}C$-methanol switch experiments at TOS = 20 min (WHSV = 2 h^{-1}) (a), TOS = 55 min (WHSV = 6 h^{-1}) (b) and TOS = 105 min (WHSV = 12 h^{-1}) (c), respectively.

during the MTO process, secondary reactions, such as the hydrogen transfer reaction, inevitably occur. In the dual-cycle mechanism (Scheme 1), the hydrogen transfer reaction connects the alkene cycle and the aromatic cycle via the generation of aromatics, MCPs and other hydrogen-poor species that function as active intermediates in the aromatic cycle. To a certain degree, then, secondary reactions (especially the hydrogen transfer reaction), are necessary for the aromatic cycle to proceed. The alkene products generated via the aromatic cycle in turn act as the intermediates for the alkene cycle and promote the activity of the alkene cycle as well. Thus the interaction between the aromatic and alkene cycles jointly promotes the overall MTO reaction.

3.5. Conversion capacity of ZSM-5 at different WHSV values

In Section 3.2, MTO reaction results showed that the initial methanol conversion increased with increasing TOS and that the maximum methanol conversion was obtained at a WHSV of 2 h^{-1}, with the lowest value at a WHSV of 12 h^{-1}. However, when the WHSV is raised, it should be considered that the methanol feed into the catalyst bed is increased. Under these conditions, catalyst penetration may be observed if the methanol feed cannot be completely converted, and the absolute amount of converted methanol will be uncertain, especially in the induction period. To exclude the effects of variations in the methanol feeding rate, the absolute amount of converted methanol normalized to the unit mass of catalyst was calculated for each trial, based on the methanol conversion and the actual WHSV of each reaction. These values were used to assess the methanol conversion capacity under different WHSV conditions (Fig. 10).

Fig. 10 shows that, after the induction period, the conversion capacity of the ZSM-5 catalyst increases as the WHSV is increased, exhibiting the opposite trend to the lowered conversion values observed in Fig. 4. During the induction period, the conversion capacities gradually increase in all the reactions, reflecting the autocatalytic nature of the process. However, in the initial period of each reaction, the sharp increase in the conversion capacity at the low WHSV shortens the induction period.

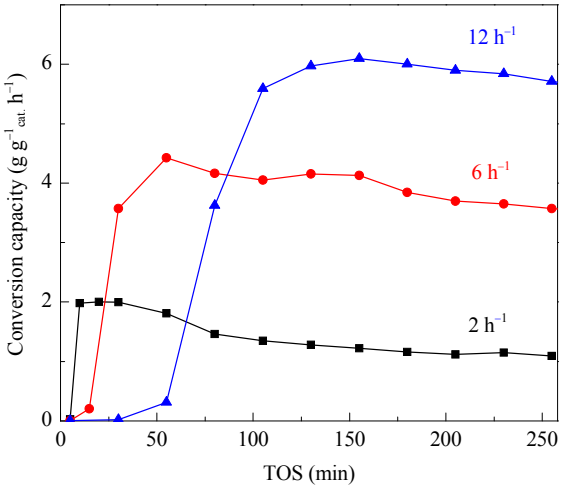

Fig. 10. Conversion capacities (absolute amounts of converted methanol over unit mass catalyst per hour) over ZSM-5 as functions of time on stream at different WHSV values.

In the case of the low WHSV reaction, the long contact time favors the hydrogen transfer reaction and promotes the rapid generation of retained organic species. The accumulation of these active aromatics is thus accelerated and the fresh zeolite is quickly transformed to a working catalyst. When employing the low WHSV, the reaction primarily proceeds via the aromatic cycle and exhibits high methanol conversion capacity in the initial reaction period. The reactions at higher WHSV values show the opposite behavior. The shorter contact times limit the extent of the hydrogen transfer reaction and suppress the generation of aromatics, lowering the conversion capacity during the initial reaction period. However, as the reaction proceeds after the induction period, a higher methanol conversion capacity is obtained, which can be attributed to the greater amount of methanol feeding and more reactants reacting with active intermediates. At the same time, the enhanced methanol conversion capacity brings about more olefin generation, and thus drives the alkene methylation and cracking reactions for methanol conversion. As demonstrated by the $^{12}C/^{13}C$-methanol switch experiments, the alkene cycle, followed by methanol conversion, is improved at higher WHSV values and lower catalyst-feedstock contact times.

4. Conclusions

MTO reactions were performed while varying the methanol WHSV value. The existence of a dual-cycle mechanism for the MTO reaction over ZSM-5 at 300 °C was confirmed by the analysis of effluent products, confined organic species and $^{12}C/^{13}C$-methanol switch experiments. It was determined that hydrogen transfer reactions could be adjusted by varying the catalyst-feedstock contact time and, in this manner, the methanol conversion reaction route (that is, whether by the aromatic cycle or alkene cycle) can be regulated. In the case of a reaction with a low WHSV, the longer time span over which the methanol contacts the catalyst bed benefits the hydrogen transfer reactions of alkene products and promotes the generation and accumulation of aromatics and MCPs on the ZSM-5 catalyst. This in turn promotes the aromatic cycle and generates ethene and aromatics among the effluents. In contrast, higher WHSV values are associated with shorter contact times that reduce the extent of the hydrogen transfer reaction and restrict the accumulation of MCPs and aromatics species. This also lowers the reactivity of the aromatic cycle and the main route of the alkene cycle in the MTO process, the C_3 to C_7 alkenes, shows more involvement in the reaction and also displays high selectivities among the effluents. Variations in the methanol-catalyst contact time also affect the accumulation of organic species and this effect further alters the dual-cycle mechanism. These findings should lead to the development of useful strategies for manipulating the MTO reaction to generate alkenes and aromatic products over the ZSM-5 catalyst.

References

[1] C. D. Chang, A. J. Silvestri, *J. Catal.*, **1977**, 47, 249–259.
[2] C. D. Chang, *Catal. Rev.-Sci. Eng.*, **1984**, 26, 323–345.
[3] Z. M. Liu, Y. Qi, *Bull. Chin. Acad. Sci.*, **2006**, 21, 406–408.
[4] P. Tian, Y. X. Wei, M. Ye, Z. M. Liu, *ACS Catal.*, **2015**, 5, 1922–1938.
[5] M. Stocker, *Microporous Mesoporous Mater.*, **1999**, 29, 3–48.
[6] U. Olsbye, S. Svelle, M. Bjorgen, P. Beato, T. V. W. Janssens, F. Joensen, S. Bordiga, K. P. Lillerud, *Angew. Chem. Int. Ed.*, **2012**, 51, 5810–5831.
[7] Y. Ono, T. Mori, *J. Chem. Soc. Faraday Trans. 1*, **1981**, 77, 2209–2221.
[8] G. J. Hutchings, F. Gottschalk, M. V. M. Hall, R. Hunter, *J. Chem. Soc. Faraday Trans. 1*, **1987**, 83, 571–583.
[9] G. A. Olah, *Pure Appl. Chem.*, **1981**, 53, 201–207.
[10] D. Kagi, *J. Catal.*, **1981**, 69, 242–243.
[11] C. D. Chang, *J. Catal.*, **1981**, 69, 244–245.
[12] D. Lesthaeghe, V. Van Speybroeck, G. B. Marin, M. Waroquier, *Angew. Chem. Int. Ed.*, **2006**, 45, 1714–1719.
[13] D. M. Marcus, K. A. McLachlan, M. A. Wildman, J. O. Ehresmann, P. W. Kletnieks, J. F. Haw, *Angew. Chem. Int. Ed.*, **2006**, 45, 3133–3136.
[14] D. Lesthaeghe, V. Van Speybroeck, G. B. Marin, M. Waroquier, *Ind. Eng. Chem. Res.*, **2007**, 46, 8832–8838.
[15] I. M. Dahl, S. Kolboe, *Catal. Lett.*, **1993**, 20, 329–336.
[16] I. M. Dahl, S. Kolboe, *J. Catal.*, **1994**, 149, 458–464.
[17] I. M. Dahl, S. Kolboe, *J. Catal.*, **1996**, 161, 304–309.
[18] D. Lesthaeghe, B. Dee Sterck, V. Van Speybroeck, G. B. Marin, M. Waroquier, *Angew. Chem. Int. Ed.*, **2007**, 46, 1311–1314.
[19] D. M. McCann, D. Lesthaeghe, P. W. Kletnieks, D. R. Guenther, M. J. Hayman, V. Van Speybroeck, M. Waroquier, J. F. Haw, *Angew. Chem. Int. Ed.*, **2008**, 47, 5179–5182.
[20] K. Hemelsoet, J. Vander Mynsbrugge, K. De Wispelaere, M. Waroquier, V. Van Speybroeck, *ChemPhysChem*, **2013**, 14, 1526–1545.
[21] X. Y. Sun, S. Mueller, Y. Liu, H. Shi, G. L. Haller, M. Sanchez-Sanchez, A. C. van Veen, J. A. Lercher, *J. Catal.*, **2014**, 317, 185–197.
[22] X. Y. Sun, S. Mueller, H. Shi, G. L. Haller, M. Sanchez-Sanchez, A. C. van Veen, J. A. Lercher, *J. Catal.*, **2014**, 314, 21–31.
[23] J. Z. Li, Y. X. Wei, J. R. Chen, P. Tian, X. Su, S. T. Xu, Y. Qi, Q. Y. Wang, Y. Zhou, Y. L. He, Z. M. Liu, *J. Am. Chem. Soc.*, **2012**, 134, 836–839.
[24] J. F. Haw, J. B. Nicholas, W. G. Song, F. Deng, Z. K. Wang, T. Xu, C. S. Heneghan, *J. Am. Chem. Soc.*, **2000**, 122, 4763–4775.
[25] T. Xu, D. H. Barich, P. W. Goguen, W. G. Song, Z. K. Wang, J. B. Nicholas, J. F. Haw, *J. Am. Chem. Soc.*, **1998**, 120, 4025–4026.
[26] S. Kolboe, *Acta Chem. Scand. Ser. A*, **1986**, A40, 711–713.
[27] W. L. Dai, C. M. Wang, X. F. Yi, A. M. Zheng, L. D. Li, G. J. Wu, N. J. Guan, Z. K. Xie, M. Dyballa, M. Hunger, *Angew. Chem. Int. Ed.*, **2015**, 54, 8783–8786.
[28] M. Hunger, W. Wang, *Chem. Commun.*, **2004**, 584–585.
[29] C. Wang, J. Xu, G. D. Qi, Y. J. Gong, W. Y. Wang, P. Gao, Q. Wang, N. D. Feng, X. L. Liu, F. Deng, *J. Catal.*, **2015**, 332, 127–137.
[30] C. Wang, X. F. Yi, J. Xu, G. D. Qi, P. Gao, W. Y. Wang, Y. Y. Chu, Q. Wang, N. D. Feng, X. L. Liu, A. M. Zheng, F. Deng, *Chem. Eur. J.*, **2015**, 21, 12061–12068.
[31] C. Wang, Q. Wang, J. Xu, G. D. Qi, P. Gao, W. Y. Wang, Y. Y. Zou, N. D. Feng, X. L. Liu, F. Deng, *Angew. Chem. Int. Ed.*, **2016**, 55, 2507–2511.
[32] C. Wang, Y. Y. Chu, A. M. Zheng, J. Xu, Q. Wang, P. Gao, G. D. Qi, Y. J. Gong, F. Deng, *Chem. Eur. J.*, **2014**, 20, 12432–12443.
[33] S. Svelle, F. Joensen, J. Nerlov, U. Olsbye, K. P. Lillerud, S. Kolboe, M. Bjørgen, *J. Am. Chem. Soc.*, **2006**, 128, 14770–14771.
[34] M. Bjørgen, S. Svelle, F. Joensen, J. Nerlov, S. Kolboe, F. Bonino, L. Palumbo, S. Bordiga, U. Olsbye, *J. Catal.*, **2007**, 249, 195–207.
[35] J. B. Wang, Y. X. Wei, J. Z. Li, S. T. Xu, W. N. Zhang, Y. L. He, J. R. Chen, M. Z. Zhang, A. M. Zheng, F. Deng, X. W. Guo, Z. M. Liu, *Catal. Sci. Technol.*, **2016**, 6, 89–97.
[36] J. R. Chen, J. Z. Li, C. Y. Yuan, S. T. Xu, Y. X. Wei, Q. Y. Wang, Y. Zhou, J. B. Wang, M. Z. Zhang, Y. L. He, S. L. Xu, Z. M. Liu, *Catal. Sci. Technol.*, **2014**, 4, 3268–3277.
[37] M. Z. Zhang, S. T. Xu, J. Z. Li, Y. X. Wei, Y. J. Gong, Y. Y. Chu, A. M. Zheng, J. B. Wang, W. N. Zhang, X. Q. Wu, F. Deng, Z. M. Liu, *J. Catal.*, **2016**, 335, 47–57.
[38] S. T. Xu, A. M. Zheng, Y. X. Wei, J. R. Chen, J. Z. Li, Y. Y. Chu, M. Z. Zhang, Q. Y. Wang, Y. Zhou, J. B. Wang, F. Deng, Z. M. Liu, *Angew. Chem. Int. Ed.*, **2013**, 52, 11564–11568.
[39] Q. Wang, Z. M. Cui, C. Y. Cao, W. G. Song, *J. Phys. Chem. C*, **2011**, 115, 24987–24992.
[40] J. Z. Li, Y. X. Wei, G. Y. Liu, Y. Qi, P. Tian, B. Li, Y. L. He, Z. M. Liu, *Catal. Today*, **2011**, 171, 221–228.
[41] J. Z. Li, Y. X. Wei, Y. Qi, P. Tian, B. Li, Y. L. He, F. X. Chang, X. D. Sun, Z.

Graphical Abstract

Chin. J. Catal., 2016, 37: 1413–1422 doi: 10.1016/S1872-2067(16)62466-X

Changing the balance of the MTO reaction dual-cycle mechanism: Reactions over ZSM-5 with varying contact times

Mozhi Zhang, Shutao Xu, Yingxu Wei *, Jinzhe Li, Jinbang Wang, Wenna Zhang, Shushu Gao, Zhongmin Liu *
Dalian Institute of Chemical Physics, Chinese Academy of Sciences; University of Chinese Academy of Sciences

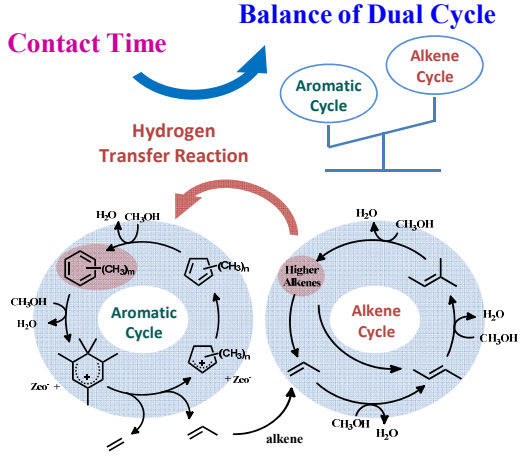

Contact time changes the balance of dual-cycle mechanism via hydrogen transfer reaction in MTH process on ZSM-5 zeolite.

M. Liu, *Catal. Today*, **2011**, 164, 288–292.
[42] S. Ilias, R. Khare, A. Malek, A. Bhan, *J. Catal.*, **2013**, 303, 135–140.
[43] S. Ilias, A. Bhan, *J. Catal.*, **2012**, 290, 186–192.
[44] D. Massiot, F. Fayon, M. Capron, I. King, S. Le Calvé, B. Alonso, J. O. Durand, B. Bujoli, Z. Gan, G. Hoatson, *Magn. Reson. Chem.*, **2002**, 40, 70–76.
[45] X. J. Li, W. P. Zhang, S. L. Liu, L. Y. Xu, X. W. Han, X. H. Bao, *J. Catal.*, **2007**, 250, 55–66.
[46] J. B. Wang, J. Z. Li, S. T. Xu, Y. C. Zhi, Y. X. Wei, Y. L. He, J. R. Chen, M. Z. Zhang, Q. Y. Wang, W. N. Zhang, X. Q. Wu, X. W. Guo, Z. M. Liu, *Chin. J. Catal.*, **2015**, 36, 1392–1402.
[47] J. Li, S. Y. Liu, H. K. Zhang, E. J. Lu, P. J. Ren, J. Ren, *Chin. J. Catal.*, **2016**, 37, 308–315.
[48] M. Guisnet, *J. Mol. Catal. A*, **2002**, 182, 367–382.
[49] M. Guisnet, L. Costa, F. R. Ribeiro, *J. Mol. Catal. A*, **2009**, 305, 69–83.
[50] W. Loewenstein, *Am. Mineral.*, **1954**, 39, 92–96.
[51] M. Hunger, *Catal. Rev.-Sci. Eng.*, **1997**, 39, 345–393.